Journal of Materials Science and Chemical Engineering, 2024, 12, 24-42
https://www.scirp.org/journal/msce
ISSN Online: 2327-6053
ISSN Print: 2327-6045

Effect of Seasonal Variations on the Behavior of Flexible Pavements in Burkina Faso: Towards Alternating and Periodic Loading of Multi-Axle Heavy Goods Vehicles for Road Durability

Kokoro Kobori[1], Doua Allain Gnabahou[1], Bouto Kossi Imbga[1,2]

[1]Laboratoire de Chimie Analytique de Physique Spatiale et Energétique, Université Norbert ZONGO, Koudougou, Burkina Faso
[2]Laboratoire d'Energie Thermique, Renouvelable, Université Joseph KI-ZERBO, Ouagadougou, Burkina Faso
Email: gnabahou@yahoo.fr

How to cite this paper: Kobori, K., Gnabahou, D.A. and Imbga, B.K. (2024) Effect of Seasonal Variations on the Behavior of Flexible Pavements in Burkina Faso: Towards Alternating and Periodic Loading of Multi-Axle Heavy Goods Vehicles for Road Durability. *Journal of Materials Science and Chemical Engineering*, **12**, 24-42.
https://doi.org/10.4236/msce.2024.126003

Received: May 12, 2024
Accepted: June 22, 2024
Published: June 25, 2024

Abstract

Bituminous materials are heat-sensitive, and their mechanical properties vary with temperature. This variation in properties is not without consequences on the performance of flexible road structures under the repeated passage of multi-axles. This study determines the influence of seasonal variations on the rate of permanent deformation, the rut depth of flexible pavements and the effect of alternating loading of heavy goods vehicles following the temperature variations on the durability of roads. Thus, an ambient and pavement surface temperature measurement was carried out in 2022. The temperature profile at different layers of the modelled pavement, the evaluation of deformation rates and rutting depth were determined using several models. The results show that the permanent deformation and rutting rates are higher at the level of the bituminous concrete layer than at the level of the asphalt gravel layer because the stresses decrease from the surface to the depth of the pavement. On the other hand, the variations in these rates, permanent deformations and ruts between the hot and so-called cold periods are more pronounced in the bitumen gravel than in bituminous concrete, showing that gravel bitumen is more sensitive to temperature variations than bituminous concrete despite its higher rigidity. Of these results, we suggested a periodic and alternating loading of the different types of heavy goods vehicles. These loads consist of fully applying the WAEMU standards with a tolerance of 15% during periods of high and low temperatures. This regulation has increased 2

to 3 times in the durability of roadways depending on the type of heavy goods vehicle.

Keywords

Pavement, Rutting, Permanent Deformation, Multi-Axle, Seasonal

1. Introduction

Bituminous materials are heat-susceptible, and their properties vary with temperature [1] [2]. The road shoes are subject to significant variations in temperature, depending on the season [3] [4] [5]. This temperature variation has a considerable impact on the rigidity of these materials [6] [7] [8]. Like most Sahelian countries, Burkina Faso presents two seasonal periods: A hot climate from March to June and a relatively cold climate from July to February. According to data from the National Meteorological Agency of Burkina Faso (ANAM) [9], the maximum ambient temperatures during the hot period reach 45˚C. In April 2022, a temperature reading on the roadway indicated 67˚C, while the minimum ambient temperatures during the cold periods ranged between 14˚C and 16˚C on the road surface [9]. Moreover, the data reveal that the thermal variation on the road surface reached 50˚C over the year. Several works have been carried out on the effect of temperature on roads. Meunier *et al.* 2012 [10], Domec *et al.* 2004 [11] and Bodin *et al.* 2014 [12]. investigated the effect of temperature on the fatigue behavior of asphalt mixes. R. KTARI *et al.* 2017 [4] worked on the thermal dependence of the fatigue performance of these asphalt mixes. At the end of their work, they suggested a study on the performance of pavements while considering seasonal temperature variations. In this paper, we aim to investigate the impact of temperature variation on the roadways in the seasonal variations context of Burkina Faso. Specifically, we evaluate the temperature variations on permanent deformations and the evolution of the rutting of materials during the life cycle of the pavement structure. Additionally, we determine the contribution of periodic alternating loading of heavy goods vehicles following climatic variations on the durability of flexible pavements within the WAEMU standard regulations.

2. Materials and Methods

2.1. Materials

The pavement structure tested consisted of bituminous concrete pavement, bitumen gravel base layer, crushed lateritic gravel foundation layer and lateritic gravel form layer on a PF3 support platform. **Figure 1** shows the structure under test. The characteristics of these layers are shown in **Table 1**.

The modules of the BB surface layer and the GB3 base layer are temperature-dependent. The road surface temperature reading was made using an infra-

red thermometer. The subdivision of the climate into two periods results from the temperature measurements from January 01 to December 31, 2022. Figure 2(a) presents the ambient, maximum, average, and minimum daily temperature, while Figure 2(b) shows pavement surface temperatures in 2022.

The traffic data and axle weighing are those obtained at the Nagréongo weighing station. Table 2 and Table 3 show the different types of multi-axle heavy goods vehicles most common on the road network of the WAEMU community. The loads defined as part of this work are those authorized by the current WAEMU standard regulations [14] [15].

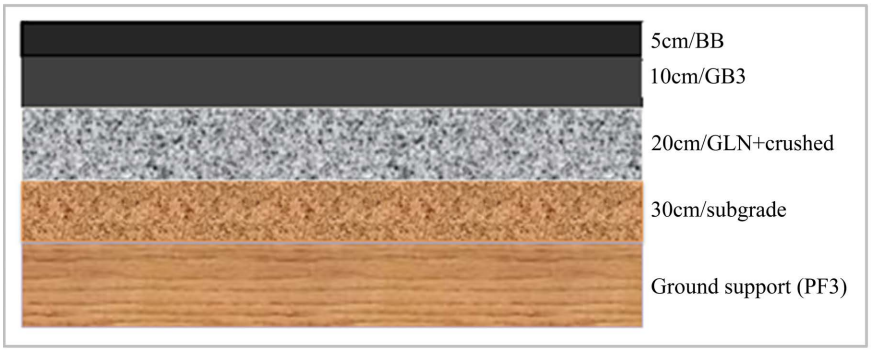

Figure 1. Pavement structure tested.

Table 1. Characteristic of the materials of the structure tested [13].

Layer	Thickness (cm)	Modulus (MPA)	Poisson's ratio coefficient
Rollover: BBSG	5	Variable	0.35
Base: GB3	12	Variable	0.35
Foundation: GLAC	20	700	0.35
Shape layer	30	200	0.35
Floor support (PF3)	Infinite	120	0.35

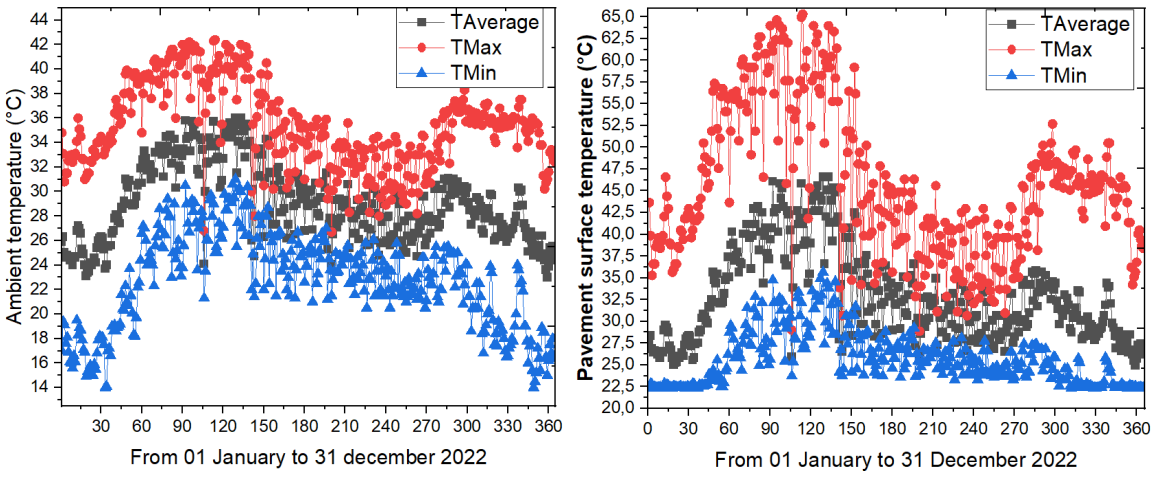

Figure 2. Minimum, average, and maximum temperature (a) of ambient air, (b) at the pavement surface.

Table 2. Permissible loading of heavy goods vehicles such as trucks P.

Coding of the main silhouettes	Number of front axles	Number of rear axles	Total number of axles	Load Currently Applied in Burkina Faso (T)	WAEMU standard (T)
Trucks P11	1	1	2	23	18
Trucks P12	1	2	3	34	26
Trucks P13	1	3	4	41	31
Trucks P22	2	2	4	41	31
Trucks P23	2	3	5	45	36
Trucks P24	2	4	6	55	42
Trucks P25	2	5	7	90	60
Trucks P26	2	6	8	90	60
Trucks P35	3	5	8	90	60

Table 3. Permissible loading of heavy goods vehicles such as Trailer TS.

Coding of the main silhouettes	Number of front axles (tractor)	Number of interme-diate axles	Number of rear axles	Total number of axles	Load Currently Applied in Burkina Faso (T)	WAEMU standard (T)
Trailer T11S2	1	1	2	4	50	38
Trailer T11S3	1	1	3	5	57	43
Trailer T11S4	1	1	4	6	66	48
Trailer T12S2	1	2	2	5	61	46
Trailer T12S3	1	2	3	6	68	51
Trailer T12S4	1	2	4	7	74	56
Trailer T12S5	1	2	5	8	90	60
Trailer T12S6	1	2	6	9	90	60

2.2. Methodology

This analysis of pavement behavior considers a multilayer structure with elastic, linear, homogeneous and isotropic behavior with static loading. [16] [17] [18]. The pavement sizing considers an average coefficient of aggressiveness equal to 1. The pavement design process ends with a mechanical evaluation, which consists of verifying the following mathematical inequalities (calculated value ≤ allowable value) [19] [20] [21]. The approach refers to the principles of the French method of pavement sizing based on a multilayer asymmetric Burmist model used in the ALIZE L C P C software [16] [22] [23] [24]. This analysis of pavement behavior considers a multilayer structure with elastic, linear, homogeneous

and isotropic behavior with static loading [16] [17] [18]. The pavement sizing takes an average aggressiveness coefficient equal to 1. The process of the design ends with a mechanical evaluation consists of verifying the satisfaction of the following mathematical inequalities (calculated value ≤ allowable value) [19] [20] [21].

For bituminous materials $\varepsilon_t \le \varepsilon_{tadm}$ (1)

For a bituminous seam stressed in bending extension, the permissible deformation is calculated through equation (2).

$$\varepsilon_{tadm} = \varepsilon_6 \times \sqrt{\left(\frac{E(10Hz;10°c)}{E(10Hz;30°c)}\right)} \times \left(\frac{NE}{10^6}\right)^b \times k_r \times k_c \times k_s \quad (2)$$

ε_t: where is Tensile deformation at the bottom of the bituminous layer

ε_{tadm}: Permissible tensile deformation at the bottom of the bituminous layer

ε_6: Deformation at 1 million loading cycles

$E(f,T(°C))$: Modulus of stiffness of asphalt layers at a temperature

NE: Number of axles equivalent to heavy goods vehicle traffic

K_r: Risk coefficient of variation in thicknesses and dispersion of fatigue tests

K_C: Calibration coefficient

K_s: coefficient that depends on the type of support platform

For untreated materials and subsoil

$$\varepsilon_z \le \varepsilon_{zadm} \quad (3)$$

For a layer of untreated material and for the soil, the permissible load is the vertical surface deformation of the layer, calculated according to equation (4)

$$\varepsilon_{zadm} = A \times (NE)^B \quad (4)$$

ε_Z: Horizontal deformation at the top of untreated layers or the platform

ε_{Zadm}: Permissible horizontal deformation at the top of the untreated layers or the platform

A: Permanent deformation

B: Slope of the Material Fatigue Law

These admissible deformation parameters are performance data of the pavement materials [16] [25]. These parameters are influenced by the type of traffic on the roadway during its lifetime [11]. The cumulative traffic was evaluated through equations 5, 6 and 7 [26] [27]. During the traffic assessment, only heavy goods vehicle traffic, expressed as the cumulative number of heavy goods vehicles expected during the lifetime of the roadway, is considered [17]. The configuration of heavy goods vehicles, which present the most aggressive elements in the traffic in Burkina Faso, has evolved rapidly, and the appearance of the multi-axle vehicle has led to the consideration of the impact on the roads of non-standard configurations following the UEMOA regulation 14 [28].

$$N_{PL} = 365 \times TMJA \times C \quad (5)$$

$$C = \frac{(1+\tau)^n - 1}{\tau} \quad (6)$$

$$NE = N_{PL} \times CAM \tag{7}$$

NE: Number of heavy goods vehicles calculated for service life

TMJA: Annual average daily traffic

n: Road life

τ: Traffic growth rate

CAM: Average coefficient of aggressiveness

The different aggressiveness is calculated using the following equations:

-The aggressiveness of an axle is given by equation 8;

$$A_i = k \times \left(\frac{P_i}{P_0} \right)^{\alpha} \tag{8}$$

-The aggressiveness of a heavy vehicle is calculated using equation (9);

$$A_{PL} = \sum_i k \times \left(\frac{P_i}{P_0} \right)^{\alpha} \tag{9}$$

-The aggressiveness of heavy goods vehicle traffic is determined by the equation (10).

$$CAM = \frac{1}{N_{PL}} \left[\sum_i \sum_{j=1}^{3} K_j n_{ij} \times \left(\frac{P_i}{P_0} \right)^{\alpha} \right] \tag{10}$$

K_j: constant dependent on axle geometry and pavement structure

α: constant dependent on the structural nature of the pavement

P_i: Axle load i

P_O: Load of the reference axle which is 13T

Since the materials that make up the pavement are considered isotropic, they are then governed by the heat equation (11) [29] [30].

The values of parameters for equations 8, 9 & 10 are those defined in the NF-P-98-086 standard [21]. These are conventional design values generally taken for sizing. In this work, only the heavy vehicle weight (HVW) or the total authorized rolling weight (TARW) according to WAEMU Regulation 14 [14] [15], in addition to the tolerance granted in October 2022 by the Ministers of Transport of the Community [15] is considered for each type of heavy good vehicles.

The mechanical behavior of asphalt concrete is largely temperature-dependent, expanding with increasing temperature and contracting with decreasing temperature. The temperature profile within the bituminous layer, as an essential parameter for this work, is determined using prediction models [31] [32].

To accurately predict pavement behavior, temperature prediction models [33] [32] [34] are required. These must predict the temperature at any pavement depth based on the ambient and surface temperature and the material properties [35] [36] [37]. As isotropic materials for the pavement, the governing heat equation (11) [29] [30] is given by:

$$\frac{\partial^2 T(x,t)}{\partial x^2} = \frac{1}{\alpha} \times \frac{\partial T(x,t)}{\partial t} \tag{11}$$

where T is the temperature, x defined the pavement Depth, t corresponding to the time and α referring to diffusivity of the material.

The pavement layer temperature was evaluated while measuring first the pavement surface temperature. An analytical approach drawn from the work of SHAO *et al.* 1999 [38] and SOLAIMANIAN *et al.* [39] has led to the development of a simple computational method requiring less raw data. This method includes the latitude effect, the location and the solar radiation. Mainly based on the equilibrium, the calculations are defined as follows [10] [38] [40].

$$q_a + q_{\bar{s}} - q_c - q_k - q_r = 0 \tag{12}$$

with

Energy from diffuse and atmospheric radiation [41] follows:

$$q_a = \varepsilon_a \times \sigma \times T_a^{\,4} \tag{13}$$

The energy absorbed by a horizontal pavement [10]:

$$qs = R_o \times \alpha_1 \times \tau_a^{\,1/\cos z} \times \cos z \tag{14}$$

The energy transmitted (or received) to the massif by convection surrounding the air [42]:

$$q_c = h_c \cdot \left(T_s - T_a\right) \tag{15}$$

The energy transmitted (or received) to the ambient air by conduction under the paving surface: $q_k = -k \cdot \left(T_x - T_s\right) \Big/ x$ (16)

The energy emitted by asphalt by radiation [33]:

$$q_r = \varepsilon \cdot \sigma \cdot T_s^{\,4} \tag{17}$$

Either, $$R_0 \times \alpha_1 \times \tau_a^{\,1/\cos z} \times \cos z + \varepsilon_a \times \sigma \times T_a^{\,4} - h_c \times \left(T_s - T_a\right) - \left(k/x\right) \times \left(T_s - T_x\right) - \varepsilon \times \sigma \times T_s^{\,4} = 0 \tag{18}$$

R_0: Solar constant

α_1: surface absorptivity

τ_a: airmass transmittance coefficient

z: angle of the Zenith (solar latitude-angle of declination)

ε_a: coefficient of atmospheric radiation

σ: Stefan-Boltzman constant

T_a: air temperature

T_s: Pavement surface temperature

T_x: temperature at depth X of the pavement

ε: emissivity factor of the pavement surface

h_c: surface area coefficient for heat transfer

k: Thermal conductivity factor

x: Pavement depth

The balance of energy exchanges is illustrated in **Figure 3**.

After determining the temperature gradient inside the different layers of the pavement, the rates of permanent deformation were obtained using equations (19) [43].

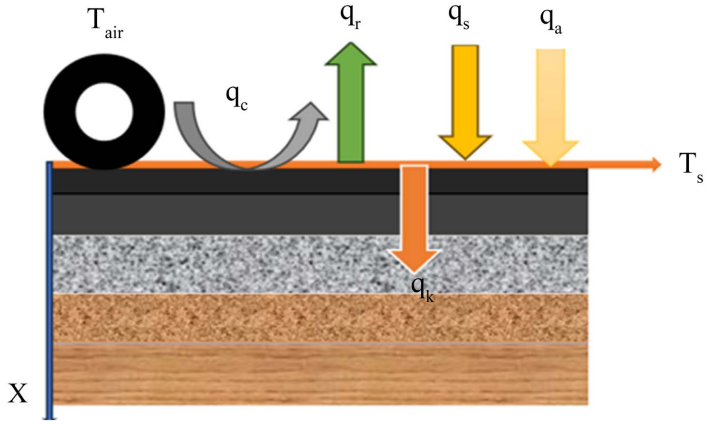

Figure 3. Illustration of energy exchanges on the pavement.

$$\varepsilon_p = \frac{\sigma_v - \sigma_h}{2.E(V,T)} \times \left[\frac{1}{450.V}\right]^{\frac{1}{4}} \times N^{\frac{1}{4}} \tag{19}$$

ε_P: Plastic deformation

N: Number of applied load

σ_v: Main vertical constraints

σ_h: Main horizontal constraints

$E(T,V)$: Modulus of stiffness of asphalt layers dependent on temperature and speed

V: Vehicle speed

And the rutted depths of the bituminous layer are evaluated through the equation (21) [43]

$$u = \sum_i h_i . \varepsilon_{pi} \tag{20}$$

μ: Rut depth

h_i: Layer thicknessi

ε_{pi}: Permanent deformation of the i-layer

3. Results and Discussions

3.1. Effect of Temperature on Permanent Deformations, Permanent Deformations of Bituminous Concrete

Figure 4 shows the evolution of permanent deformations on the asphalt concrete layer by month and for a cumulative 20 years. From Figures 4(a), Figure 4 (c) and Figure 4(e), it is clear that the permanent deformations are higher during March, April, May and June and smaller during January, February, July, August, September and December. A rebound of these deformations was observed during October. In Figure 4(a) and Figure 4(b), the deformation rates of multi-axle heavy trucks indicate that the P25, P26 and P35 trucks generate higher deformation rates than other types of trucks. Figure 4(c) and 4d show the deformation rates of twin-axle semi-trailers. For these types of heavy trucks, the difference in deformation rates is insignificant. In Figure 4(e) and Figure 4(f),

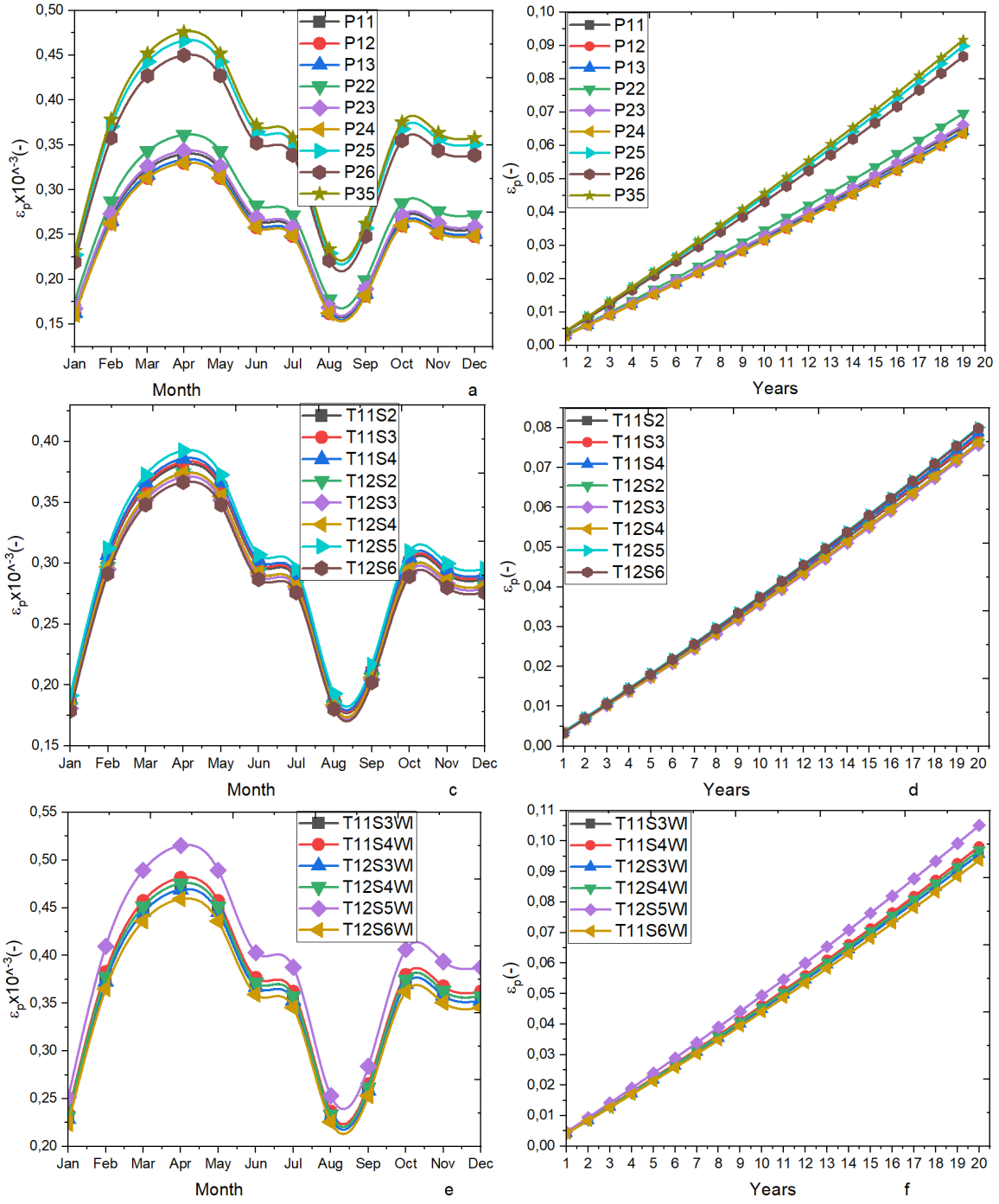

Figure 4. Effect of temperature on permanent deformations of asphalt concrete for a year and over 20 years. (a) and (b) under the loads of heavy goods vehicles of the truck type P, (c) and (d) under the loads of heavy goods vehicles semi-trailers with twin wheels, (e) and (f) under the loads of heavy goods vehicles semi-trailers with single wheels.

which represent the deformation rates of heavy goods vehicles such as semi-trailers with isolated rear axles, the value recorded for the T12S5 with single axles is higher than those of the other types of heavy goods vehicles shown in these figures. Our finding is consistent with the work of BASSEM *et al.* (2006) [44], which showed that single axles cause more damage to the

pavement than twin axles. All the figures here show that the T12S5 semi-trailers with single axles contribute more to permanent deformation, followed by the P25, P26 and P35 type trucks and all semi-trailers with twin axles. P11, P12, P13, P22, P23 and P24 truck types contribute less to deformations. These results complete our previous work (KOBORI *et al.* (2023)) [45], which indicates that heavy goods vehicles were the most aggressive cause of permanent deformation.

3.2. Effect of Temperature on Permanent Deformations, Permanent Deformations of Gravel Bitumen

Figure 5 shows the permanent deformations of the gravel bitumen's seam under the stresses of the various heavy goods vehicles over the course of a year (**Figure 5(a)**, **Figure 5(c)** and **Figure 5(e)**.) and over 20 years (**Figure 5(b)**, **Figure 5(d)**. and **Figure 5(f)**). In general, it appears that the same heavy goods identified as being the most contributors to the rate of permanent deformation at the level of the bituminous concrete layer also turn out to be the most severe in the asphalt gravel layer. These permanent deformations in the gravel bitumen layer (**Figure 5**) are less significant than in the asphalt concrete layer (**Figure 4**) because gravel bitumen is stiffer than asphalt concrete.

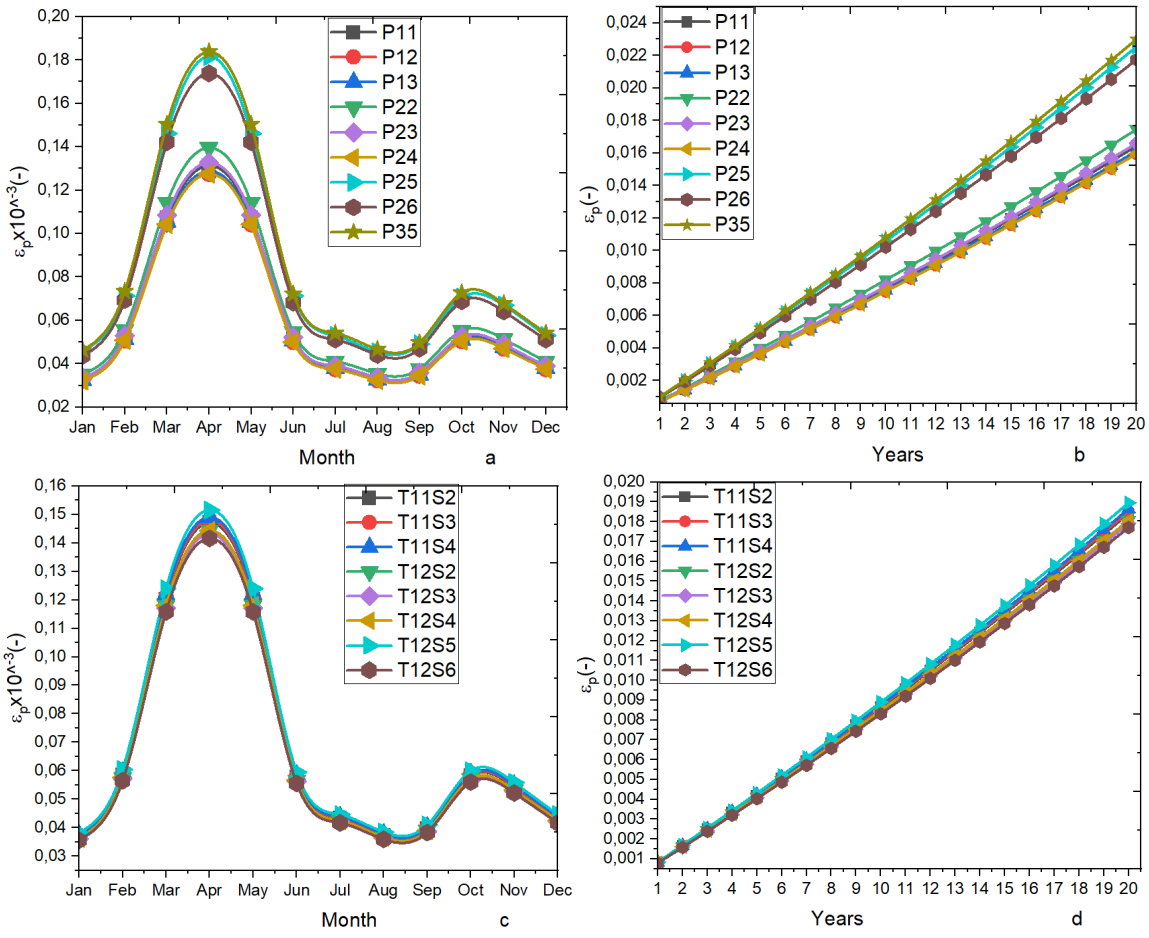

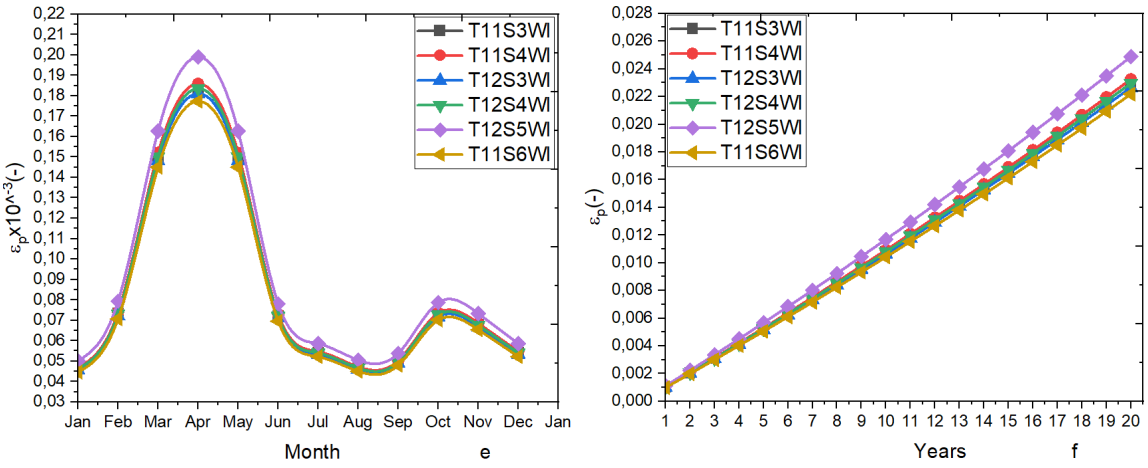

Figure 5. Effect of temperature on permanent deformations of gravel bitumen for a year and over a period of 20 years. (a) and (b) under the loads of heavy goods vehicles of the type P, (c) and (d) under the loads of heavy goods vehicles semi-trailers with twin wheels, (e) and (f) under the loads of heavy goods vehicles semi-trailers with single wheels..

On the other hand, in terms of seasonal variation, the gravel bitumen layer experiences more variation in permanent deformation than the asphalt concrete layer. The difference in these deformations between the warm and cold periods is more pronounced in the case of gravel bitumen than in bituminous concrete since bitumen is more sensitive to temperature variation than asphalt concrete [6] [40] [46].

3.3. Effect of Temperature on Pavement Rutting

3.3.1. Rutting of the Bituminous Concrete Layer

Figure 6 shows the effect of temperature over a year on the appearance of ruts and the accumulation of these ruts 20 years on the bituminous concrete layer, under the stress of heavy trucks with multi-axles. By referring to **Figure 6(a)**, **Figure 6(c)** and **Figure 6(e)**, the rutting depth appears higher during the warm period, consistent with existing results in the literature [44] [47] [48]. It is twice as large during the hot period as the cold one, under stress from all types of heavy goods vehicles.

The cumulative rutting depth is greater than 5 mm for single-wheel semi-trailers and P25, P26 and P35-type trucks. For dual-wheel semi-trailers, it is of 4 mm order and less than 3.5 mm for P11, P12, P13, P22, P23 and P24 type trucks.

3.3.2. Rutting of the Gravel Bitumen's Layer

Figure 7 shows the rutting depths generated on the gravel bitumen for a year (**Figure 7(a)**, **Figure 7(c)** and **Figure 7(e)**) and the cumulative rutting for 20 years (**Figure 7(b)**, **Figure 7(d)** and **Figure 7(f)**) under multi-axle loads. A comparison with the results in **Figure 6** shows that the rutting depth is two times higher for the asphalt concrete level than that of asphalt gravel by the stress levels and temperature in the gravel bitumen, which are lower than those of asphalt concrete. We also observe that gravel bitumen gives sharp peaks of

ruts during the hot period due to the very high sensitivity of this material to temperature. These results confirm the work of R.F DOLIN *et al.* (2021) [49], which showed that temperature plays a role in the ruts formation in flexible pavements.

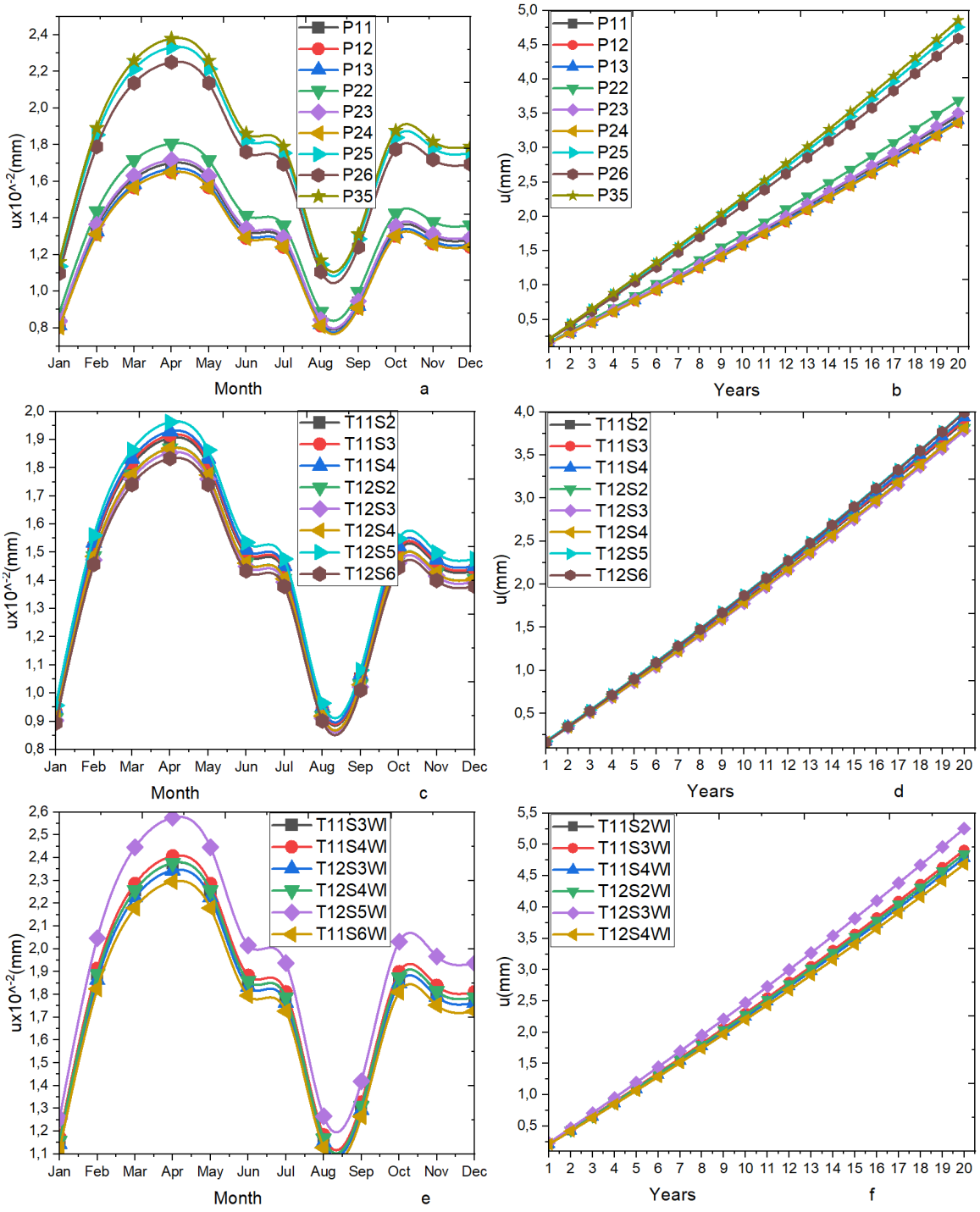

Figure 6. Effect of temperature on rutting of the asphalt concrete layer for a year and over a 20-year period. (a) and (b) under the loads of heavy goods vehicles such as trucks P, (c) and (d) under the loads of heavy goods vehicles semi-trailers with twin wheels, (e) and (f) under the loads of heavy goods vehicles semi-trailers with single wheels.

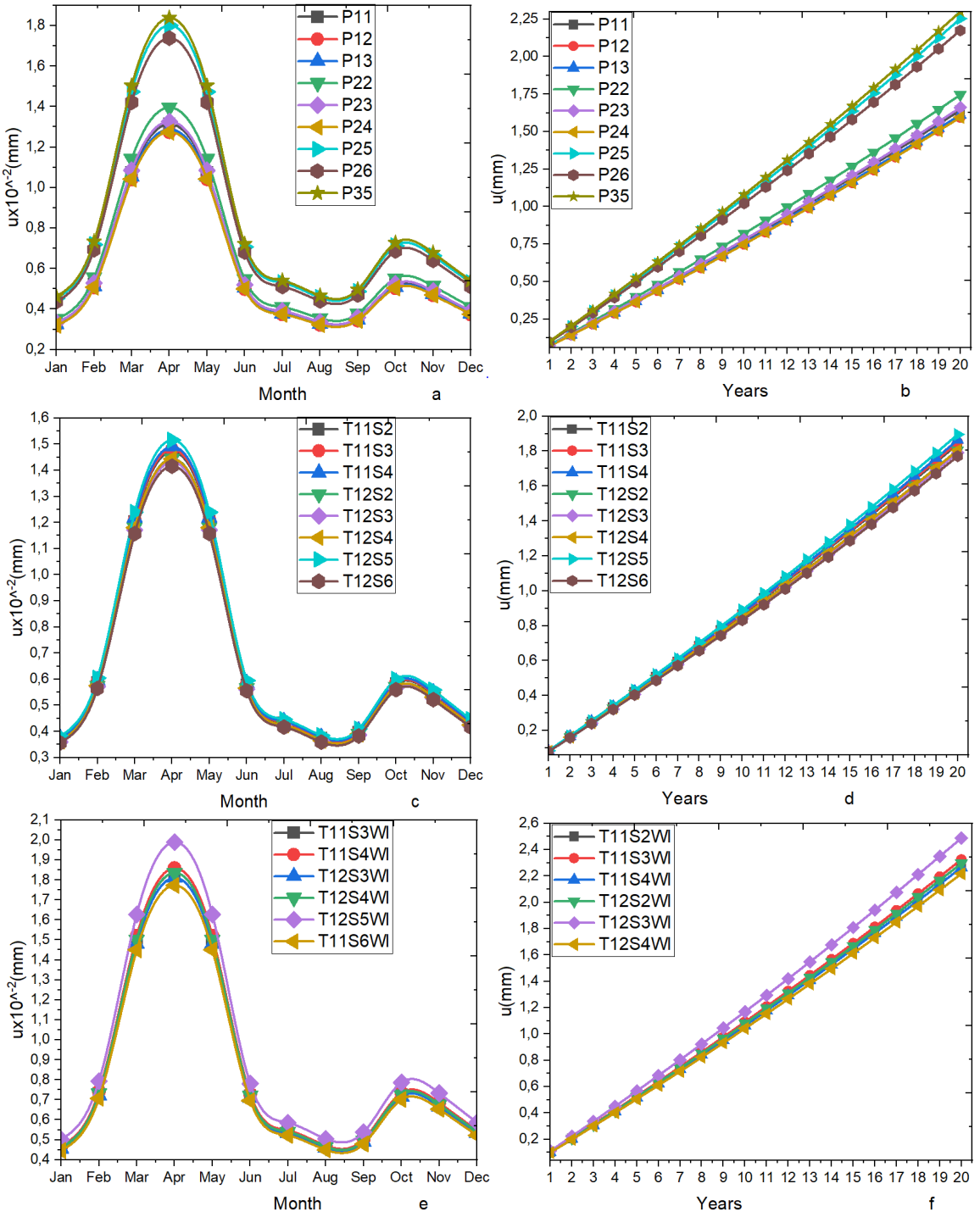

Figure 7. Effect of temperature on gravel rutting for a year and over 20 years. (a) and (b) under the loads of heavy goods vehicles such as trucks P, (c) and (d) under the loads of heavy goods vehicles semi-trailers with twin wheels, (e) and (f) under the loads of heavy goods vehicles semi-trailers with single wheels.

3.4. Impact of Periodic and Alternating Loading of Heavy Goods Vehicles on the Life of the Bituminous Layer

Figure 8 illustrates the durability of a bituminous seam under multi-axle loads as a function of three types of loading. Loading in compliance with WAEMU

Regulation 14 [14] [15]; then a loading following the recommendations of the Ministers of Transport of the WAEMU Community Area with the tolerance of 15% overload and to an alternating loading during a year which consists of a loading in compliance with Regulation 14 during the so-called hot season and a loading following the recommendations for the cold period. The results of the simulation show that alternating loading can double the durability of the bituminous layer under the stresses of heavy goods vehicles such as P25, P26 and P35. This lifetime of the bituminous layer is tripled for the full application of WAEMU Regulation 14 (**Figure 8(a)**) [14] [15]. The same finding was observed in **Figure 8(b)**. **Figure 8(c)** shows the durability of the bituminous layer under loads of heavy semi-trailers with insulated wheels as a function of load. Consequently, the road life is tripled for alternating loading and quadrupled for loading following the entire application of the WAEMU standard for a year. However, it is pointed out that the work was based on the French method of sizing pavements. This is a method that does not include cracks in pavements. If the analysis of the results showed that the flexible pavement is vulnerable in high temperatures. Because during this period, rutting formation and deformation

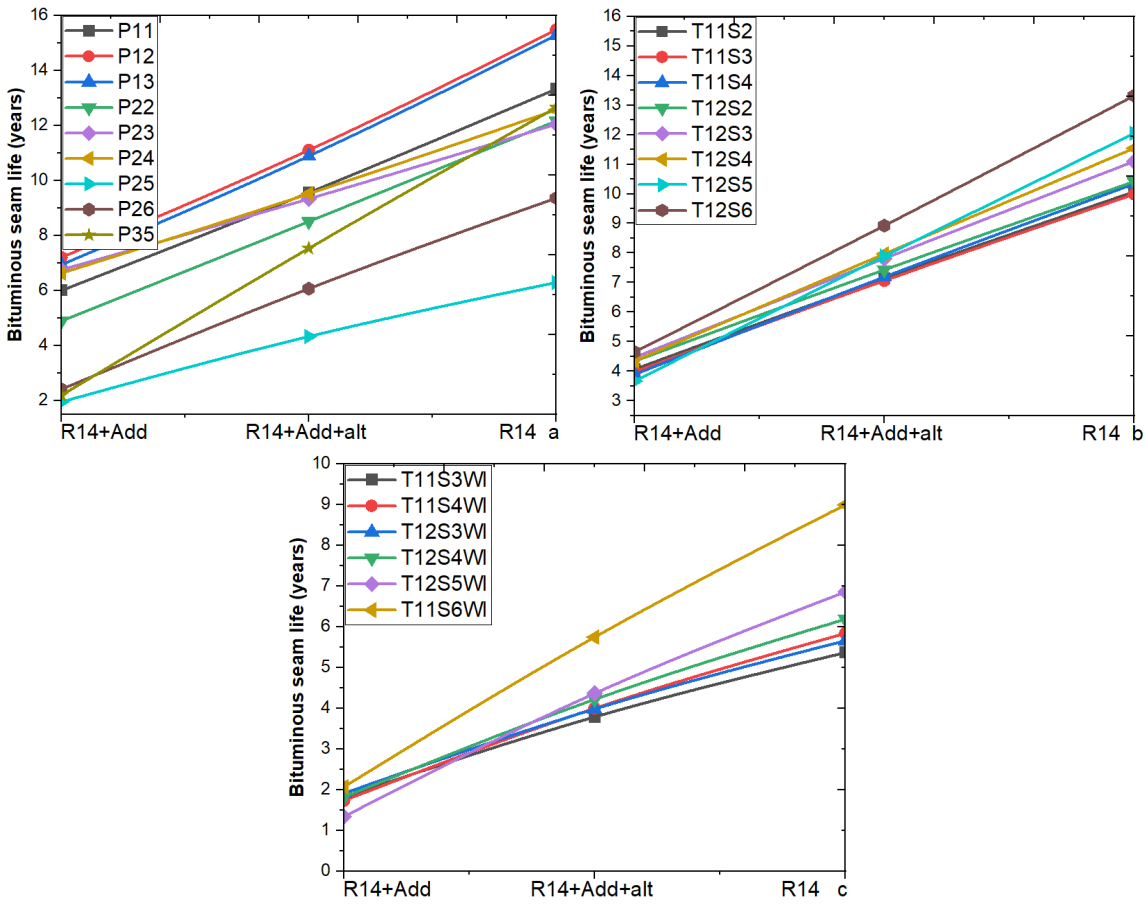

Figure 8. Impact of periodic and alternating loading of heavy goods vehicles on the service life of the bituminous seam. (a) under the loads of heavy goods vehicles of the P truck type, (b) under the loads of heavy goods vehicles semi-trailers with twin wheels, (c) under the loads of heavy goods vehicles semi-trailers with single wheels.

rates are higher. Several studies have also shown that periods of low temperature are also harmful to the road. These studies have shown that this so-called cold period is favourable to the formation of cracks on flexible pavements. [50] [51]

3.5. Impact of Periodic and Alternating Heavy Truck Loading on the Service Life of Granular Materials

Figure 9 shows the evolution of the durability of granular materials as a function of multi-axle heavy truck loading. From this figure, the durability of these materials increases by 1.5 times for seasonal alternating loading and more than three times the loading according to WAEMU Regulation 14 [14] for heavy trucks of P25, P26 and P35 types (**Figure 9(a)**). There has also been a significant change in the durability of materials for alternating loading under the load of multi-axle semi-trailers with twin wheels (**Figure 9(b)**). **Figure 9(c)** shows that the durability of granular materials is multiplied by two for seasonal alternating loading and more than three times for loading complying with WAEMU standards under the stresses of semi-trailers with insulated wheels. Although the properties are insensitive to temperature variations, the durability of granular materials increases

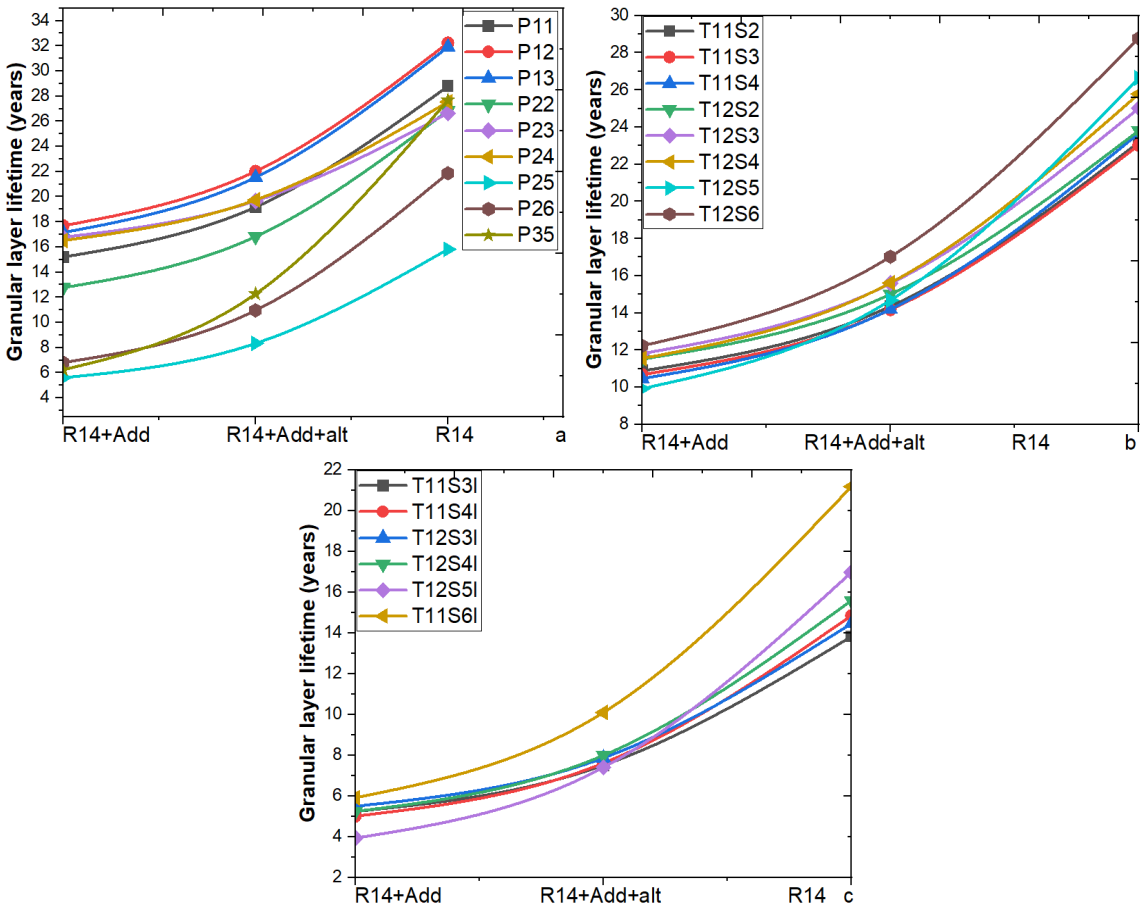

Figure 9. Impact of alternating heavy truck loading on the service life of the bituminous layer. (a) under the loads of heavy goods vehicles of the P truck type, (b) under the loads of heavy goods vehicles semi-trailers with twin wheels, (c) under the loads of heavy goods vehicles semi-trailers with single wheels.

with the alternation of loading due to the variation in the stress levels resulting from the decrease in the stiffness of the bituminous layer. These results are acceptable because the period from July to October is considered cold and wet in Burkina Faso. However, studies have shown that the strength of granular materials decreases with humidity. This period can then be detrimental to granular materials [47].

4. Conclusion

This paper discusses the impact of seasonal variations on the behavior of flexible pavements. It also discusses the effect of alternating loading of heavy goods vehicles following this seasonal variation on the durability of the pavement. The results show that the period from March to June, the hottest of the year in Burkina Faso, is the key contributor in terms of rutting depth and permanent deformation rates under the load of multi-axle heavy goods vehicles. By proposing alternating loading of heavy goods vehicles, which consists of applying a load according to WAEMU regulation 14 during periods of high temperature and the rest of the year, the loading is according to the recommendations of the Ministers of Transport of the WAEMU area, namely an overload tolerance, it is possible to increase the durability of the pavements by two times under the stresses of the most aggressive heavy trucks. As for a strict application of WAEMU Regulation 14, the durability of the pavement is multiplied by more than 3 to 4 times under the same type of heavy goods vehicle loads. For perspective, it is desirable to complete this work with a study that integrates the impact of seasonal variations on pavement cracking and considers the effect of capillary rise in granular materials.

Acronyms

R14 + Add: loading of heavy goods vehicles according to the recommendations of the WAEMU transport ministers for a surface tolerance of 15%

R14 + Add + Alt: loading of heavy goods vehicles according to the recommendations of the Ministers of Transport of the WAEMU area for a surface tolerance of 15% during the so-called cold period and during the hot period full application of WAEMU Regulation 14.

R14: Loading in full accordance with WAEMU Regulation 14. Loading in full accordance with WAEMU Regulation 14.

Conflicts of Interest

The authors declare no conflicts of interest regarding the publication of this paper.

References

[1] Ali, B. (2007) Modèle numérique pour comportement mécanique des chaussées: Application à l'analyse de l'orniérage. Universite des Sciences et Technologies de Lille, Lille. http://www.univv-lille1.fr/bustl

[2] Olard, F. (2005) Loithermo-visco-elastique-plastique pour les enrobés bitumineux simulations des essais de traction directe et de retrait thermique empéché. 15-39.

[3] Mauduit, V., *et al.* (2013) Dégradation subite des enrobés bitumineux par période de gel/dégel: Analyse de cas de terrain et recherche exploratoire en laboratoire. *Bulletin de Liaison des Laboratoires des Ponts et Chaussées*, **279**, 47-63.

[4] Rahma, K., Hornych, P., Hammoum, F. and Marsac, P. (2017) Dépendance thermique des performances en fatigue des enrobés bitumineux. https://www.researchgate.net/publication/323393938%0A

[5] Tran, D.T. (2021) Endommagement des enrobés bitumineux soumis à des cycles de gel/dégel.

[6] Bodin, D., Hornych, P. and Marsac, P. (2010) Effect of Temperature on Fatigue Performances of Asphalt Mixes.

[7] Pambou, C.H.K. (2013) Developpement D'Un Catalogue de Conception des Chaussées Pour Les Pays Sub-Sahariens.

[8] Afechkar, M. (2005) La fatigue des enrobes bitumineux, impact de la température et de la nature des granulats.

[9] ANAM (2023) temperature annulle de 1993 à 2022.

[10] Meunier, M. (2012) Prédiction de l'ornierage lié aux deformations permanentes des enrobés bitumineux. Université du Québec, Québec.

[11] Domec, V., *et al.* (2016) Caractérisation de la durée de vie en fatigue des enrobés bitumineux en conditions de « trafic simulé » et de température Caractérisation de la durée de vie en fatigue des enrobés bitumineux en conditions de « trafic simulé » et de température. Vol. 7120.

[12] Bodin, D. (2019) Modele d'endommagement cyclique: Application à la fatigue des enrobés bitumineux.

[13] SETRA and LCPC (1998) Catalogue des structures types de chaussées neuves.

[14] UEMOA (2005) A Règlement n°14/2005/CM/UEMOA relatif à l'harmonisation des normes et des procédures du contrôle du gabarit, du poids, et de la charge à l'essieu des véhicules lourds de transport de marchandises dans les états membres de l'union Economique et Monétaire O.

[15] UEMOA (2022) Réunion des ministres en charges des infrastructures et de transports routiers des Etats membres de L'UEMOA pour l'application intégrale et concomitante du Règlement n°14/2005/CM/UEMOA du 16 décembre 2005 relatif à l'harmonisation des normes et des procéd.

[16] Ambassa, Z., Allou, F., Petit, C. and Eko, R.-M. (2011) Modélisation viscoélastique de l'endommagement des chaussées bitumineuses sous essieux multiples. 120-129.

[17] Ambassa, Z., Allou, F., Petit, C. and Medjo Eko, R. (2013) Evaluation de l'agressivite du trafic sur des chaussees bitumineuses en carrefour giratoire. *Bulletin de liaison des laboratoires des ponts et chaussées*, No. 280-281, 171-188.

[18] Teresa, L. and Mart, A.H. (2022) The Effect of Temperature, Rest Periods and Age-ing on the Response of Bituminous Materials in Fatigue Tests: Considerations and Proposals on Analytical Dimensioning Models.

[19] A. et AIPCR (2019) Revue du guide pratique de dimensionnement des chaussees pour les pays tropicaux.

[20] Laurent, D.S. (2021) Dimensionnement structural des chaussees souples au MTQ logiciel CHAUSSEE2. Québec.

[21] NF-P-98-086-2011 (2011) Dimensionnement-structurel-des-chaussées-routières

Application aux chaussées neuves.

[22] Manuel d'utilisation du logiciel ALIZÉ-LCPC (2010).

[23] N.E.A.T. Adolphe Kimbonguila, Frederic Becquart (2015) Méthode de dimensionnement des structures de chaussées: Quelle(s) adaptabilité(s) pour les matériaux granulaires alternatifs? https://hal.archives-ouvertes.fr/hal-01167601

[24] Duong, N.S. (2017) Instrumentation de chaussées: La route intelligente qui s'autodétecte?

[25] Mengue, E., *et al.* (2015) Dimensionnement d'une assise de chaussée à base d'un sol latéritique traité au ciment à différents dosages. 33*èmes Rencontres l'AUGC; ISABTP/ UPPA*, Anglet, 27-29 mai 2015.

[26] Perre, J. and Dumont, A.-G. (2004) Modélisation des charges d'essieu. Ecole Polytechnique Fédérale de Lausanne (EPFL).

[27] Babilotte, C. and Soulie Cete, C. (2009) Guide technique de conception et de dimensionnement des structures de chaussées communautaires. Guid. Tech. https://www.spfrq.qc.ca

[28] Dgnet (2020) Données_comptage_trafic_du réseau routier du Burkina Faso de 1993 à 2019.

[29] Marc, P.T. (2011) Conception et réalisation de structures Routières a hautes performances. 1-73.

[30] Han, R., Jin, X., Glover, C.J. and Ph, D. (2011) Modeling Pavement Temperature for Use in Binder Oxidation Models and Pavement Performance Prediction. *Journal of Materials in Civil Engineering*, **23**, 351-359. https://doi.org/10.1061/(ASCE)MT.1943-5533.0000169

[31] Park, D., Buch, N. and Chatti, K. (1986) Model and Temperature Correction via Falling Weight Deflectometer Deflections.

[32] Hermansson, Å. (1998) Mathematical Model for Calculation of Pavement Temperatures.

[33] Inge, A. (1997) Simplified Procedure for Prediction of Asphalt Pavement Subsurface Temperatures. Paper No. 971509.

[34] Yahia, C. and Yahia, J.C. (2012) Validation d'un modèle physique de prévision de la température de surface du revêtement de la chaussée: Intégration de données *in Situ* et de prévisions à moyenne échéance pour l'élaboration d'informations en météorologie routière hivernale. https://tel.archives-ouvertes.fr/tel-00688806

[35] Kim, H.B., Buch, N. and Park, D. (2000) Mechanistic-Empirical Rut Prediction Model for In-Service Pavements. *Transportation Research Record*, **1730**, 99-109.

[36] Somé, S.C. (2013) Comportement thermomécanique des enrobés tièdes et de l'interface bitume-granulat. Université de Nantes, Nantes.

[37] M.S.A.T.W.K. (1993) Asphalt Concrete Mixtures Predicting Maximum Pavement Surface Temperature Using Maximum Air Temperature and Hourly Solar Radiation Mansour. No. 1417.

[38] Hermansson, Å. (2000) Simulation Model for Calculating Pavement Temperatures Including Maximum Temperature. *Transportation Research Record*, **1699**, 134-141. https://doi.org/10.3141/1699-19

[39] Solaimanian, M. (1993) Predicting Maximum Pavement Surface Temperature Using Maximum Air Temperature and Hourly Solar Radiation.

[40] Hornych, P. (2015) Effets de la temperature sur le dimensionneemt des chaussées. https://www.cerema.fr

[41] Bliss, R.W. (1961) Atmospheric Radiation near the Surface of the Ground: A Summary for Engineers. *Solar Energy*, **5**, 103-120.

[42] Koudougou, S.M. and Toguyeni, D.Y.K. (2020) Modeling of Pavement Behavior in Tropical Hot and Dry Conditions: Numerical Approach and Comparison on Road Section. *Journal of Materials Science & Surface Engineering*, **7**, 919-927.

[43] Perret, J. (2003) Déformations des couches bitumineuses au passage d'une charge de traffic. Vol. 2786, p. 263.

[44] Perron-Drolet, F. (2015) Effets des changements climatiques sur la performance à long terme des chaussées souples au Québec. Laval.

[45] Kobori, K., Gnabahou, D.A., Imbga, K. and Sandwidi, A.S. (2023) Impact of Multi-Axle Vehicles and Road Overloads on the Durability of Asphalt Pavements. *Open Journal of Civil Engineering*, **13**, 237-251. https://doi.org/10.4236/ojce.2023.132018

[46] Badiane, M. (2016) Effet des charges sur les chausses en priode de restriction des charges-volet terrain. Maître ès sciences, Université de Laval, Laval.

[47] Sohm, J. and Sohm, J. (2013) Prédiction des déformations permanentes des matériaux bitumineux. https://tel.archives-ouvertes.fr/tel-00777561

[48] Breysse, D., Homsi, F., Yotte, S., Balay, J. and Bodin, D. (2013) Utilisation du manège dans la construction d'un modèle de fatigue des chaussée sous chargement multi-essieux. *Rev. Générale des Routes l'aménagement* 2, **914**-**915**, 87-92.

[49] Dolin, R.F., Ramroson, M., Rabevala, R., Arnolev, R.Z. and Richar, R.T. (2021) Modelization Thermo-Mechanical Behavior of Soft Pavement Applied to the Prediction of Ordering of the Base Treated with Local Vegetable Binders. *American Journal of Innovative Research and Applied Sciences*, **12**, 138-144.

[50] Laveissiere, D. (2002) Modélisation de la remontée de fissure en fatigue dans les structures routières par endommagement et macro-fissuration De l'expérimentation a l'outil de dimensionnement pour l'estimation de la durée de vie. Thèse de doctorat, Universite de Limoges, Limoges.

[51] Perraton, D., Di, H., Carter, A. and Proteau, M. (2019) Link between Different Bottom-Up Fatigue's Law Coefficients of Mechanical-Empirical Pavement Design Software. *Construction and Building Materials*, **216**, 552-563. https://doi.org/10.1016/j.conbuildmat.2019.04.256